

Green functions simulation of the energy and charge transfer between highly charged ions and 2D materials

Michael Bonitz, Karsten Balzer, Hannes Ohldag, Jan-Philip Joost

Institute for Theoretical Physics and Astrophysics, Kiel University
in collaboration with Anna Niggas and Richard Arthur Wilhelm, TU Vienna

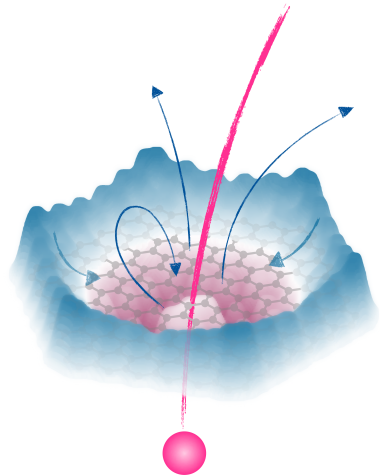


DPG Frühjahrstagung

Dresden, March 2023

pdf at <http://www.theo-physik.uni-kiel.de/bonitz/talks.html>

- Experiments with highly charged ions at TU Vienna (R. Wilhelm)
- Xe^{40+} ion penetrates monolayers of graphene and MoS_2
- ultrafast emission of slow electrons into vacuum: ca. 80 per ion, **6 times more electrons released from graphene** \Rightarrow sensitive local probe of electronic properties
- **theoretical explanation?**
suitable approaches?



¹A. Niggas *et al.*, Phys. Rev. Lett. **129**, 086802 (2022), Editors' Choice

- time-dependent many-electron Hamiltonian

$$H(t) = \underbrace{\sum_{i=1}^N h(\mathbf{r}_i, t)}_{\text{one-body operators}} + \frac{1}{2} \underbrace{\sum_{i \neq j}^N W(\mathbf{r}_i, \mathbf{r}_j)}_{\text{pair-wise interactions}}$$

- time-dependent Schrödinger equation (TDSE)

$$i\partial_t \Psi(\mathbf{r}_1, \dots, \mathbf{r}_N; t) = H(t) \Psi(\mathbf{r}_1, \dots, \mathbf{r}_N; t)$$

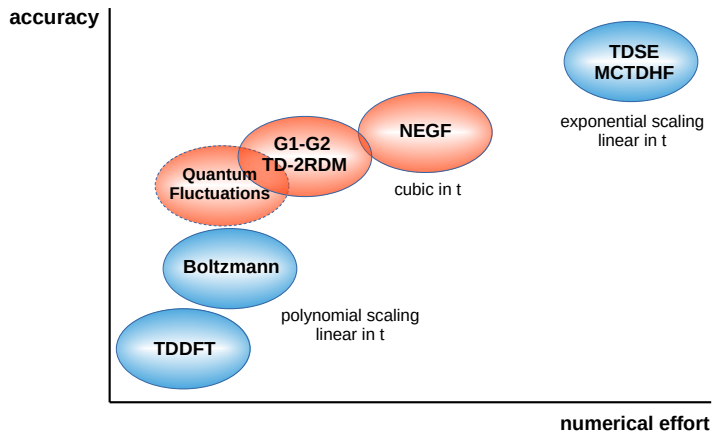
direct solution
↯
 $\Psi(\mathbf{r}_1, \dots, \mathbf{r}_N; t)$

exponential scaling of numerical effort

- solutions to overcome exponential scaling:**

- approximations to TDSE: TD-RASCI, TD-CASSCF, truncated CC, TD-R-matrix etc.
 D. Hochstuhl and M. Bonitz, PRA (2012) and EJP-ST (2014), embedding techniques
- propagation of **simpler observables**: density (TDDFT), **distribution function (Kinetic theory)**, **correlation functions etc.**

- NEGF:** systematically captures electronic correlations, scattering, on all time scales
but: computationally expensive. Complementary to TDDFT
- G1–G2 scheme:** acceleration of NEGF, time-linear scaling



Nonequilibrium Green Functions (NEGF)

2nd quantization

- Fock space $\mathcal{F} \ni |n_1, n_2 \dots\rangle$, $\mathcal{F} = \bigoplus_{N_0 \in \mathbb{N}} \mathcal{F}^{N_0}$, $\mathcal{F}^{N_0} \subset \mathcal{H}^{N_0}$
- $\hat{c}_i, \hat{c}_i^\dagger$ creates/annihilates a particle in single-particle orbital ϕ_i
- spin accounted for by canonical (anti-)commutator relations

$$\left[\hat{c}_i^{(\dagger)}, \hat{c}_j^{(\dagger)} \right]_{\mp} = 0, \quad \left[\hat{c}_i, \hat{c}_j^\dagger \right]_{\mp} = \delta_{i,j}$$
- Hamiltonian:
$$\hat{H}(t) = \underbrace{\sum_{k,m} h_{km}^0 \hat{c}_k^\dagger \hat{c}_m}_{\hat{H}_0} + \frac{1}{2} \underbrace{\sum_{k,l,m,n} w_{klmn} \hat{c}_k^\dagger \hat{c}_l^\dagger \hat{c}_n \hat{c}_m}_{\hat{W}} + \hat{F}(t)$$

Particle interaction w_{klmn}

- Coulomb interaction
- electronic correlations

Time-dependent excitation $\hat{F}(t)$

- single-particle type
- em field, quench, particles

Nonequilibrium Green Functions (NEGF)

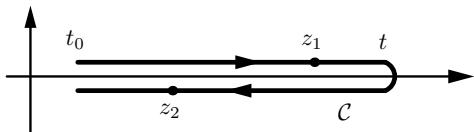
two times $z, z' \in \mathcal{C}$ ("Keldysh contour"), arbitrary one-particle basis $|\phi_i\rangle$

$$G_{ij}(z, z') = \frac{i}{\hbar} \langle \hat{T}_{\mathcal{C}} \hat{c}_i(z) \hat{c}_j^\dagger(z') \rangle \quad \text{average with } \hat{\rho}_N$$

pure or mixed state

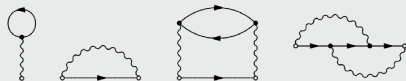
Keldysh–Kadanoff–Baym equations (KBE) on \mathcal{C} (2×2 matrix):

$$\sum_k \left\{ i\hbar \frac{\partial}{\partial z} \delta_{ik} - h_{ik}(z) \right\} G_{kj}(z, z') = \delta_{\mathcal{C}}(z, z') \delta_{ij} - i\hbar \sum_{klm} \int_{\mathcal{C}} d\bar{z} w_{iklm}(z^+, \bar{z}) G_{lmjk}^{(2)}(z, \bar{z}; z', \bar{z}^+)$$



KBE: first equation of Martin–Schwinger hierarchy for $G, G^{(2)} \dots G^{(n)}$

- $\int_{\mathcal{C}} w G^{(2)} \rightarrow \int_{\mathcal{C}} \Sigma G$, Selfenergy
- Nonequilibrium Diagram technique
 Example: Hartree–Fock + Second Born selfenergy



- Correlation functions G^{\lessgtr} obey real-time KBE

$$\sum_l \left[i\hbar \frac{d}{dt} \delta_{i,l} - h_{il}^{\text{eff}}(t) \right] G_{lj}^>(t, t') = I_{ij}^{(1),>}(t, t'),$$

$$\sum_l G_{il}^<(t, t') \left[-i\hbar \frac{d}{dt'} \delta_{l,j} - h_{lj}^{\text{eff}}(t') \right] = I_{ij}^{(2),<}(t, t'),$$

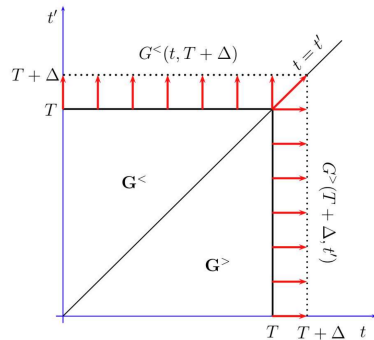
with the effective single-particle **Hartree–Fock Hamiltonian**

$$h_{ij}^{\text{eff}}(t) = h_{ij}^0 \pm i\hbar \sum_{kl} w_{ikjl}^{\pm} G_{lk}^<(t)$$

and the collision integrals

$$I_{ij}^{(1),>}(t, t') := \sum_l \int_{t_s}^{\infty} d\bar{t} \left\{ \Sigma_{il}^R(t, \bar{t}) G_{lj}^>(\bar{t}, t') + \Sigma_{il}^>(t, \bar{t}) G_{lj}^A(\bar{t}, t') \right\},$$

$$I_{ij}^{(2),<}(t, t') := \sum_l \int_{t_s}^{\infty} d\bar{t} \left\{ G_{il}^R(t, \bar{t}) \Sigma_{lj}^<(\bar{t}, t') + G_{il}^<(t, \bar{t}) \Sigma_{lj}^A(\bar{t}, t') \right\}.$$



$$\mathcal{O}(N_t^3)$$

- two-time structure contains **spectral information**
- numerically demanding due to **cubic scaling with number of time steps N_t**

Hartree–Fock (HF, mean field): $\sim w^1$

Second Born (2B): $\sim w^2$

GW: ∞ bubble summation,
dynamical screening effects

particle-particle T -matrix (TPP):

∞ ladder sum in pp channel

particle-hole T -matrix (TPH/TEH):

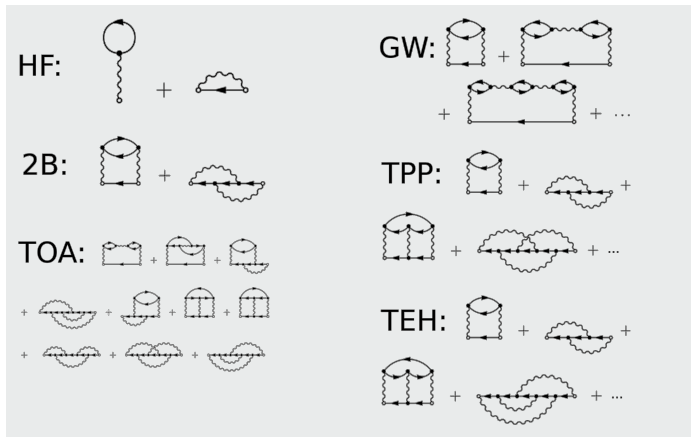
∞ ladder sum in ph channel

3rd order approx. (TOA): $\sim w^3$

dynamically screened ladder (DSL)*:

$\sim 2B + GW + TPP + TPH$

Choice depends on coupling strength, density (filling)

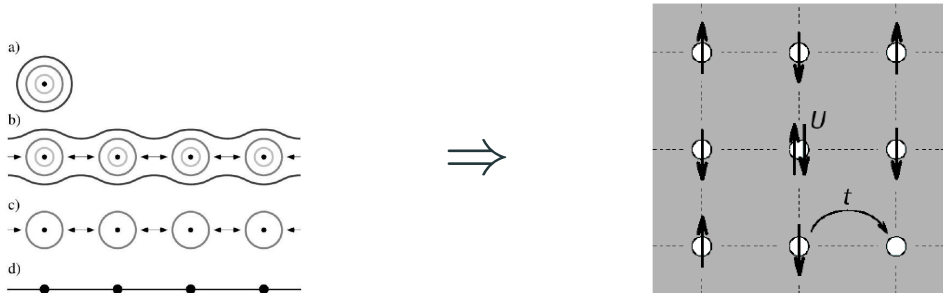


²Conserving approximations, nonequilibrium $\Sigma(t, t')$, applies for ultra-short to long times

Review: Schlünzen *et al.*, J. Phys. Cond. Matt. **32**, 103001 (2020); *Joost *et al.*, PRB (2022)

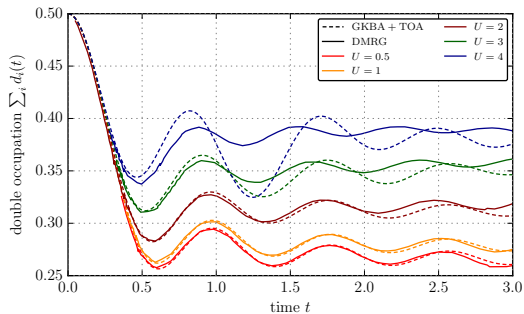
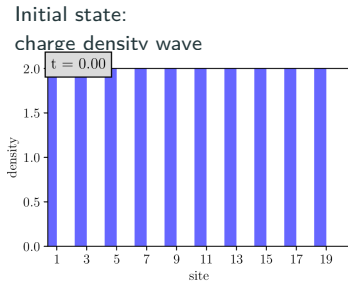
Testing various selfenergies: the Hubbard model

- Simple, but versatile model for strongly correlated solid state systems, 2D materials
- Suitable for single band, small bandwidth; atoms in optical lattices



$$\hat{H}(t) = J \sum_{ij, \alpha} h_{ij} \hat{c}_{i\alpha}^\dagger \hat{c}_{j\alpha} + U \sum_i \hat{c}_{i\uparrow}^\dagger \hat{c}_{i\uparrow} \hat{c}_{i\downarrow}^\dagger \hat{c}_{i\downarrow} + \sum_{ij, \alpha\beta} f_{ij, \alpha\beta}(t) \hat{c}_{i\alpha}^\dagger \hat{c}_{j\beta}$$

- $h_{ij} = -\delta_{\langle i, j \rangle}$ nearest neighbor hopping, on-site repulsion ($U > 0$) or attraction ($U < 0$),
- f : external single-particle potential: e.g. potential quench, laser field, ion impact
- parameters from electronic structure calculations (DFT) or experiment
- can be systematically improved: extended Hubbard and PPP model, multiple bands

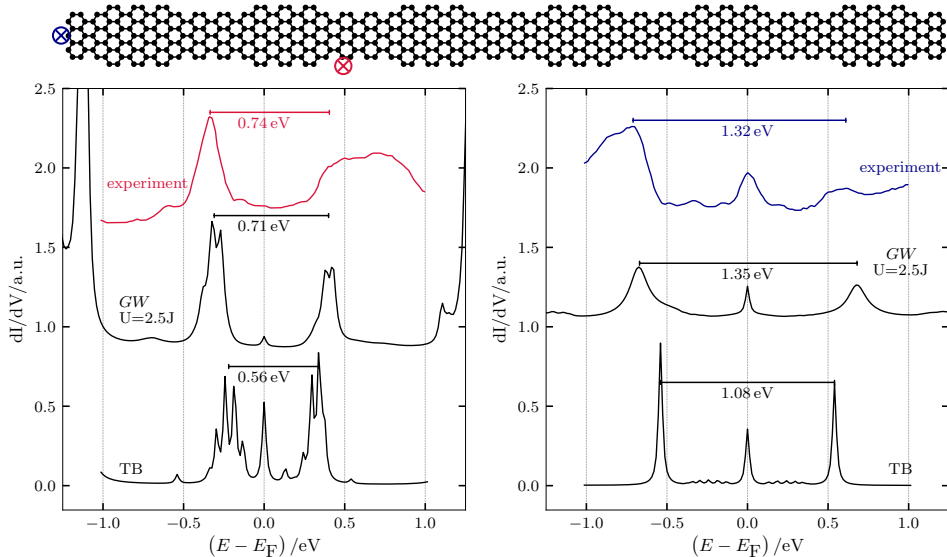


- sensitive observable: total double occupation
- good quality transients NEGF up to $U \simeq$ bandwidth
- accurate long-time behavior of GKBA+T-matrix (not shown)
- performance of different selfenergies vs. coupling and filling³

³N. Schlünzen, S. Hermanns, M. Scharnke, and M. Bonitz, J. Phys.: Cond. Matt. 32 (10), 103001 (2020)

⁴N. Schlünzen, J.-P. Joost, F. Heidrich-Meisner, and M. Bonitz, Phys. Rev. B 95, 165139 (2017)

Local density of states of graphene nanoribbons: Bulk vs. End



Failure of tight binding and Hartree-Fock. **Excellent agreement of NEGF-GW: electronic correlations crucial**
Experiments: Rizzo et al. Nature, **560**, 204 (2018), NEGF simulations: Joost et al. Nano Lett. **19**, 9045 (2019)

- **full propagation** on the time diagonal ($I := I^{(1),<}$):

$$i\hbar \frac{d}{dt} G_{ij}^{<}(t) = [h^{\text{HF}}, G^{<}]_{ij}(t) + [I + I^\dagger]_{ij}(t)$$

- **reconstruct off-diagonal NEGF** from time diagonal:

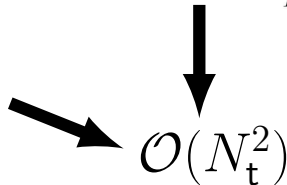
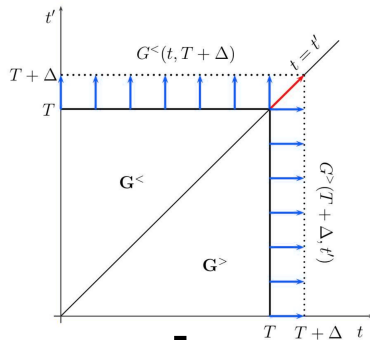
$$G_{ij}^{\geq}(t, t') = \pm \left[G_{ik}^{\text{R}}(t, t') \rho_{kj}^{\geq}(t') - \rho_{ik}^{\geq}(t) G_{kj}^{\text{A}}(t, t') \right]$$

$$\text{with } \rho_{ij}^{\geq}(t) = \pm i\hbar G_{ij}^{\geq}(t, t)$$

- HF-GKBA: use Hartree–Fock propagators for $G_{ij}^{\text{R/A}}$

$$G_{ij}^{\text{R/A}}(t, t') = \mp i\Theta_{\mathcal{C}}(\pm[t - t']) \exp\left(-\frac{i}{\hbar} \int_{t'}^t d\bar{t} h_{\text{HF}}(\bar{t})\right) \Big|_{ij}$$

- conserves total energy



⁶ P. Lipavský, V. Špička, and B. Velický, Phys. Rev. B **34**, 6933 (1986);
 K. Balzer and M. Bonitz, Lecture Notes in Physics **867** (2013)

- **full propagation** on the time diagonal as for ordinary HF-GKBA:

$$i\hbar \frac{d}{dt} G_{ij}^<(t) = [h^{\text{HF}}, G^<]_{ij}(t) + [I + I^\dagger]_{ij}(t)$$

- but collision integral defined by correlated two-particle Green function

$$I_{ij}(t) = \pm i\hbar \sum_{klp} w_{iklp}(t) \mathcal{G}_{lpjk}(t)$$

- which obeys an ordinary differential equation

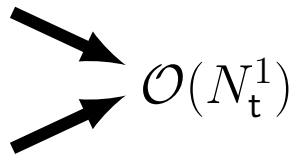
$$i\hbar \frac{d}{dt} \mathcal{G}_{ijkl}(t) = [h^{(2),\text{HF}}, \mathcal{G}]_{ijkl}(t) + \Psi_{ijkl}^\pm(t)$$

- the initial values

$$G_{ij}^{0,<} = \pm \frac{1}{i\hbar} n_{ij}(t_0) =: \pm \frac{1}{i\hbar} n_{ij}^0,$$

$$\mathcal{G}_{ijkl}^0 = \frac{1}{(i\hbar)^2} \{ n_{ijkl}^0 - n_{ik}^0 n_{jl}^0 \mp n_{il}^0 n_{jk}^0 \},$$

determine the density and the pair correlations existing in the system at the initial time $t = t_0$



⁶N. Schlünzen, J.-P. Joost, and M. Bonitz, Phys. Rev. Lett. **124**, 076601 (2020)

- other selfenergy approximations can be reformulated in the G1–G2 scheme in similar fashion:⁷

$$i\hbar \frac{d}{dt} \mathcal{G}_{ijkl}(t) = \left[h^{(2),\text{HF}}(t), \mathcal{G}(t) \right]_{ijkl} + \Psi_{ijkl}^{\pm}(t) + \underbrace{L_{ijkl}(t)}_{\text{TPP}} + \underbrace{P_{ijkl}(t)}_{\text{GW}} \pm \underbrace{P_{jikl}(t)}_{\text{TPH}}$$

$$L_{ijkl} := \sum_{pq} \left\{ \mathfrak{h}_{ijpq}^L \mathcal{G}_{pqkl} - \mathcal{G}_{ijpq} \left[\mathfrak{h}_{klpq}^L \right]^* \right\}, \quad \mathfrak{h}_{ijkl}^L := (i\hbar)^2 \sum_{pq} \left[\mathcal{G}_{ijpq}^{\text{H},>} - \mathcal{G}_{ijpq}^{\text{H},<} \right] w_{pqkl},$$

$$P_{ijkl} := \sum_{pq} \left\{ \mathfrak{h}_{qjpl}^{\Pi} \mathcal{G}_{piqk} - \mathcal{G}_{qjpl} \left[\mathfrak{h}_{qkpi}^{\Pi} \right]^* \right\}, \quad \mathfrak{h}_{ijkl}^{\Pi} := \pm (i\hbar)^2 \sum_{pq} w_{qipk}^{\pm} \left[\mathcal{G}_{jplq}^{\text{F},>} - \mathcal{G}_{jplq}^{\text{F},<} \right]$$

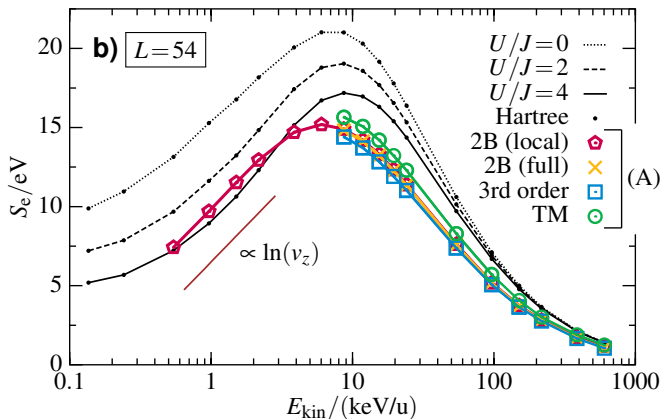
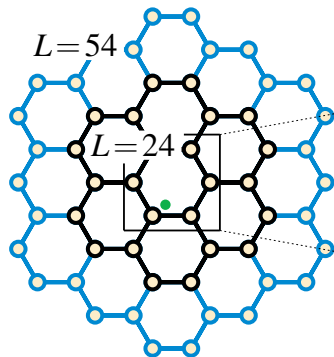
and the Hartree/Fock (H/F) two-particle Green functions

$$\mathcal{G}_{ijkl}^{\text{H},\gtrless}(t) := G_{ik}^{\gtrless}(t,t) G_{jl}^{\gtrless}(t,t), \quad \mathcal{G}_{ijkl}^{\text{F},\gtrless}(t) := G_{il}^{\gtrless}(t,t) G_{jk}^{\gtrless}(t,t)$$

- include TPP, GW and TPH terms simultaneously: dynamically-screened-ladder (DSL) approximation. Conserving, applicable to short times. No explicit selfenergy known.⁸
- nonequilibrium generalization of ground state result (Bethe-Salpeter equation)

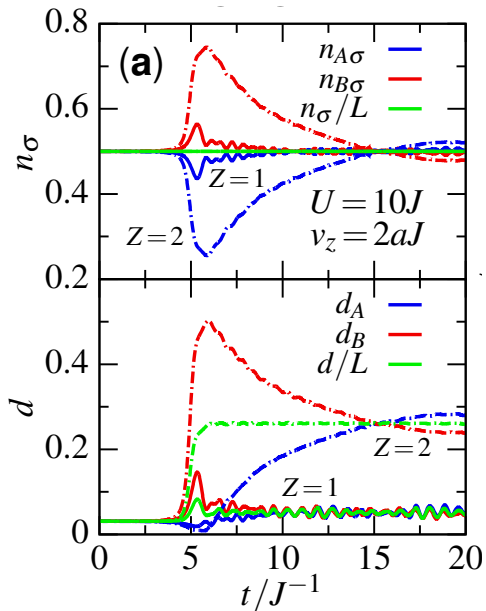
⁷ J.-P. Joost, N. Schlünzen, and M. Bonitz, PRB **101**, 245101 (2020), Joost et al., PRB **105**, 165155 (2022);

⁸ J.-P. Joost, PhD thesis, Kiel University 2023



Left: finite honeycomb cluster and impact point of ion (green). Right: Ion energy loss S_e vs. impact energy. Black lines: Hartree approximation for e-e interaction. Colors: different approximations for the correlation selfenergy. Electron correlations generally reduce stopping, except for low impact energy.

From: K. Balzer, N. Schlünzen, and M. Bonitz PRB **94**, 245118 (2016)



Central impact of proton (full lines) or α -particle (at $t = 6J$) in honeycomb cluster of 12 sites.

B: inner ring, A: outer ring, mean

Top: electron density dynamics. Mean density constant, only redistribution (green)

Bottom: doublon number. Ion causes increase of doublon number (electronic excitation), remains in cluster after impact (before dissipation to lattice). Spreads uniformly across cluster.

From: Balzer *et al.* PRL **121**, 267602 (2018)

Physical system (s) embedded in ("large") environment (e) that is treated in simplified manner

$$\Omega = \{s, e\} : \quad H_{\text{total}} = \sum_{\alpha\beta \in \Omega} \sum_{ij} h_{ij}^{\alpha\beta}(t) c_i^{\alpha\dagger} c_j^{\beta} + \frac{1}{2} \sum_{\alpha\beta\gamma\delta \in \Omega} \sum_{ijkl} w_{ijkl}^{\alpha\beta\gamma\delta} c_i^{\alpha\dagger} c_j^{\beta\dagger} c_k^{\gamma} c_l^{\delta}.$$

$$\text{NEGF, density matrix : } G_{ij}^{\alpha\beta}(t, t') = -i \langle T_C c_i^{\alpha}(t) c_j^{\beta\dagger}(t') \rangle, \quad \rho_{ij}^{\alpha\beta}(t) = -i G_{ji}^{\beta\alpha}(t, t^+),$$

Keldysh-Kadanoff-Baym equations of total system including coupling (se) terms:

$$\left\{ i\partial_t \delta_{ik} - h_{ik}^{\text{HF},s}(t) \right\} G_{kj}^s(t, t') = h_{ik}^{\text{HF},se}(t) G_{kj}^{es}(t, t') + \delta_{ij} \delta_C(t, t') + \int_C d\bar{t} \Sigma_{ik}^s(t, \bar{t}) G_{kj}^s(\bar{t}, t').$$

$$\left\{ i\partial_t \delta_{ik} - h_{ik}^{\text{HF},e}(t) \right\} G_{kj}^{es}(t, t') = h_{ik}^{\text{HF},es}(t) G_{kj}^s(t, t'),$$

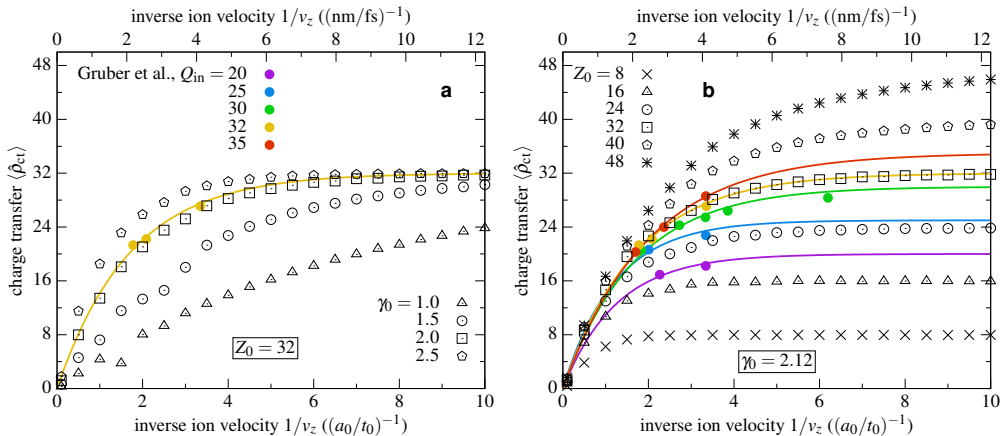
$$\left\{ i\partial_t \delta_{ik} - h_{ik}^{\text{HF},e}(t) \right\} G_{kj}^e(t, t') = \delta_{ij} \delta_C(t, t').$$

Effect of environment can be rewritten as additional selfenergy to retain closed equation for G^s :

$$\Sigma_{ij}^{\text{emb}}(t, t') = \sum_{kl} h_{ik}^{\text{HF},se}(t) G_{kl}^e(t, t') h_{lj}^{\text{HF},es}(t'), \quad h_{ij}^{\text{se}}(t) = \int d^3r \phi_i^{s*}(\vec{r}) (T + V) \chi_j^e(\vec{r}; t).$$

Appl. to resonant charge transfer: Bonitz *et al.*, Front. Chem. Sciences Engin. **13**, 201-237 (2019)

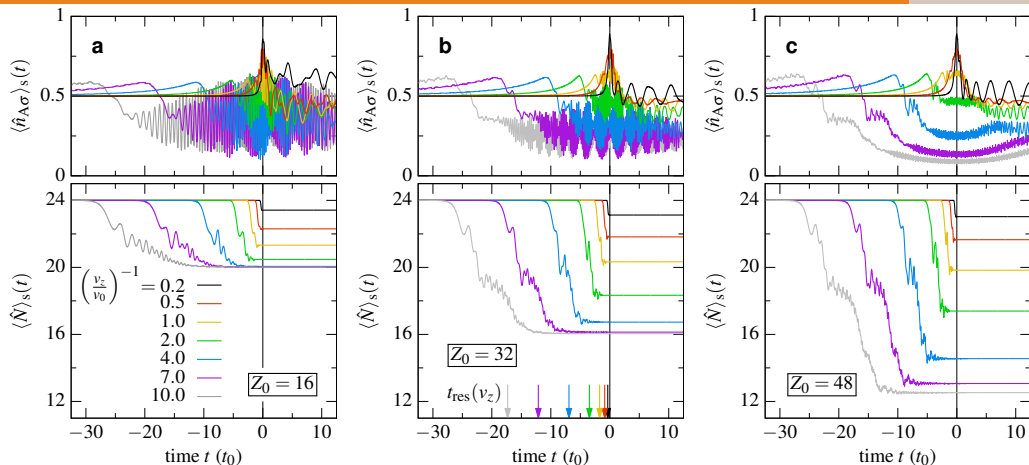
NEGF-embedding scheme for charge transfer from graphene nanoflake to impacting high- Z ion



NEGF-embedding selfenergy scheme for resonant charge transfer, $L = 24$. Exp. data from Gruber et al. Nat. Commun. 2016, **7**(1), 13948. Single adjustable parameter γ_0 works for all charges.

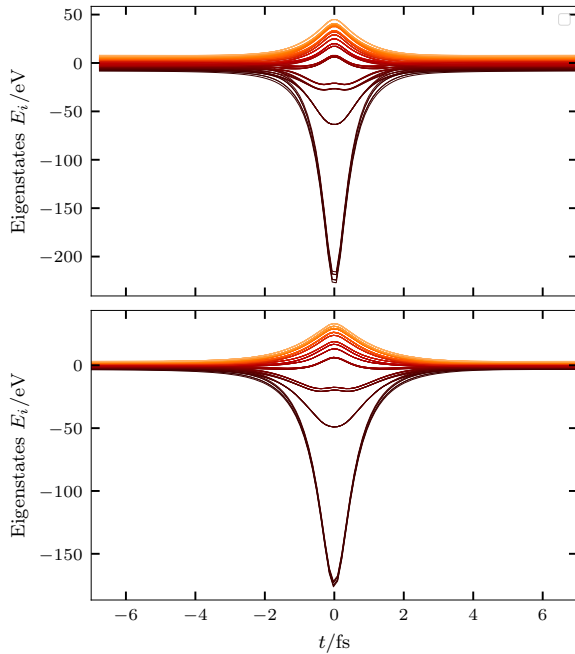
Figure from Balzer and Bonitz, Contrib. Plasma Phys. **62** (2) e202100041 (2022)

Charge transfer from graphene nanoflake to impacting high- Z ion

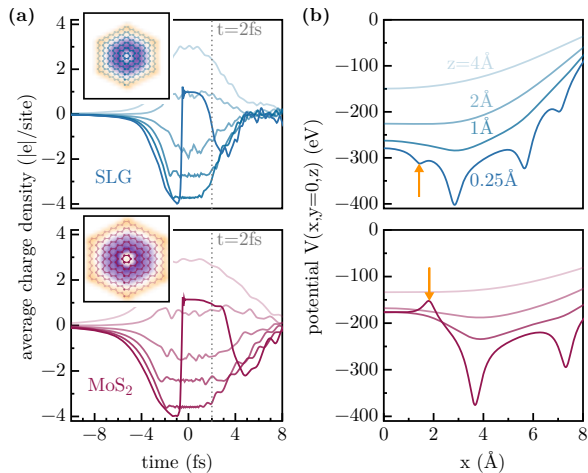


Bottom: total particle number (in one band) and Top: occupation of innermost honeycomb (graphene, $L = 24$ sites) during ion impact. Colors: NEGF results for different ion velocities. Arrows: moment when ion passes through the resonance point $z_{res} = \sqrt{3}a_0$, in front of the plane. From Balzer and Bonitz, Contrib. Plasma Phys. **62** (2) e202100041 (2022).

Energy eigenvalues during ion impact (top: SLG, bottom: MoS₂)

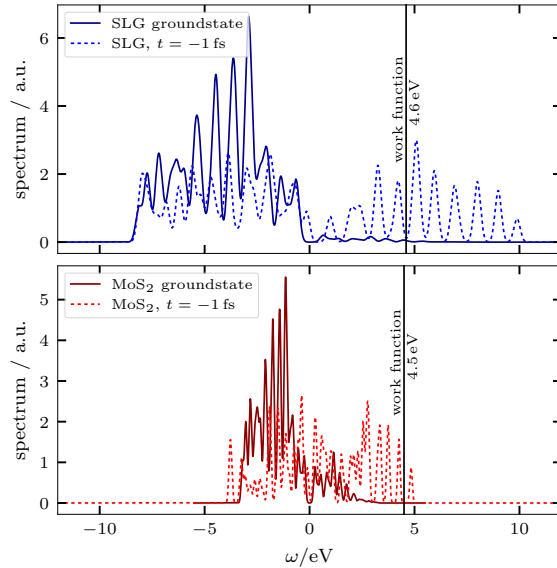


Local density dynamics (a) and electrostatic potential after ion impact



(a) time resolved radial electron density. (b) Induced electrostatic potential, $V(\mathbf{r}, t)$ at $t = 2$ fs, versus radial coordinate x , at four distances z from the monolayer. The arrows indicate the position of the innermost honeycomb from which electron emission is expected to occur primarily. 113 keV Xe³²⁺ ions passing through the center of a 216-site cluster. Niggas. *et al.*, Phys. Rev. Lett. **129**, 086802 (2022)

Energy spectrum without ion and directly before impact



G1-G2 scheme (SOA selfenergy): 113 keV Xe³²⁺ ion, graphene: $J = 2.8eV$, $U/J = 1.6$, $a_L = 1.42\text{\AA}$
MoS₂: $J = 1.1eV$, $U/J = 4.0$, $a_L = 1.83\text{\AA}$, Niggas. et al., Phys. Rev. Lett. **129**, 086802 (2022)

- Exciting novel experiments with highly charged ions and graphene/TMDC monolayers
- NEGF simulations well suited to follow dynamics of electronic correlations with single-site resolution on (sub-)fs time scale
- advanced selfenergies capture key electronic excitation processes; require electronic structure theory (DFT) input for accurate lattice model or proper basis sets.
- Neutralization via resonant charge transfer modeled using a NEGF embedding selfenergy approach.
- G1–G2 calculations allow for long and efficient simulations (linear in time)⁹
- Outlook: - combine embedding concept with G1–G2 scheme: arXiv:2211.09615 (PRB 2023)
 - improved description of ion
 - embedding approach to Auger processes and ICD

⁹ N. Schlünzen, J.-P. Joost and M. Bonitz, Phys. Rev. Lett. **124**, 076601 (2020)

J.-P. Joost, N. Schlünzen, and M. Bonitz, Phys. Rev. B **101**, 245101 (2020)

J.-P. Joost, N. Schlünzen, H. Ohldag, M. Bonitz, F. Lackner, and I. Brezinova, Phys. Rev. B **105**, 165155 (2022)